

## $\beta$ -Turn Modified Gramicidin S Analogues Containing Arylated Sugar Amino Acids Display Antimicrobial and Hemolytic Activity Comparable to the Natural Product

Gijsbert M. Grotenbreg,<sup>†,‡</sup> Annelies E. M. Buizert,<sup>†</sup> Antonio L. Llamas-Saiz,<sup>‡</sup> Emile Spalburg,<sup>§</sup> Peter A. V. van Hooft,<sup>||</sup> Albert J. de Neeling,<sup>§</sup> Daan Noort,<sup>||</sup> Mark J. van Raaij,<sup>‡</sup> Gijsbert A. van der Marel,<sup>†</sup> Herman S. Overkleeft,<sup>\*,†</sup> and Mark Overhand<sup>\*,†</sup>

Contribution from the Leiden Institute of Chemistry, Gorlaeus Laboratories, P.O. Box 9502, 2300 RA Leiden, The Netherlands, Unidad de Rayos X (RIAIDT), Laboratorio Integral de Dinámica y Estructura de Biomoléculas "José R. Carracido", Edificio CACTUS, Campus Sur, Universidad de Santiago de Compostela, 15782 Santiago de Compostela, Spain, National Institute of Public Health and the Environment, Research Laboratory for Infectious Diseases, P.O. Box 1, 3720 BA Bilthoven, The Netherlands, and TNO, Prins Maurits Laboratory, P.O. Box 45, 2280 AA Rijswijk, The Netherlands

Received December 31, 2005; E-mail: h.s.overkleeft@chem.leidenuniv.nl; overhand@chem.leidenuniv.nl

**Abstract:** This paper describes the design and synthesis of gramicidin S (GS) analogues **10a–c** containing arylated sugar amino acids (SAAs) as a replacement of one of the two <sup>D</sup>Phe-Pro  $\beta$ -turn regions. The cyclic, amphiphilic peptides adopt a  $\beta$ -sheet conformation featuring an unusual reverse turn induced by the SAAs. The altered turn region induces a slight distortion of the antiparallel  $\beta$ -sheet, as compared to GS; the overall geometry however closely resembles that of the nonarylated GS analogue **1**. GS analogues **10a–c** proved to be as active as the parent GS itself as antibacterial agents and are equally efficient in lysing red blood cells. These properties are in sharp contrast to the diminished biological activity displayed by **1**. We conclude that the presence of aromaticity in the turn regions of GS derivatives is required for biological activity, whereas the native conformation of the beta-hairpin is not. Our findings may guide future research toward efficient and nonhemolytic GS analogues for combating bacterial infections.

### Introduction

Gramicidin S (GS, Figure 1) is an amphiphilic cyclic decapeptide having the  $C_2$ -symmetrical sequence *cyclo*(Pro-Val-Orn-Leu-<sup>D</sup>Phe)<sub>2</sub> that acts as an antibiotic by targeting the membrane lipid bilayer.<sup>1,2</sup> Upon accumulation into the lipid bilayer, GS induces lysis with bacterial cell death as the ultimate result. The ability of GS to interact with the bacterial membrane is attributed to its amphiphilic nature, with the two basic Orn residues occupying one side of the cyclic peptide and the aliphatic Leu and Val residues located at the opposite side. The amphiphilicity of GS is enhanced by its adoption of an antiparallel  $\beta$ -sheet.<sup>3</sup> This conformation is stabilized by four intramolecular hydrogen bonding interactions at the opposing

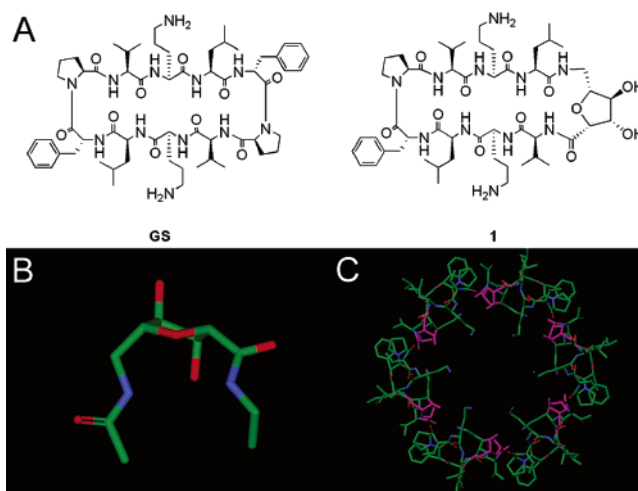


**Figure 1.** (A) Structures of gramicidin S and SAA-modified GS analogue **1**. (B) The SAA residue in **1** and (C) the  $\beta$ -barrel-like assembly of **1** in the X-ray structure.

Leu and Val residues and two hydrophobic type II'  $\beta$ -turns with the <sup>D</sup>Phe-Pro dipeptide stretches holding the  $i + 1$  and  $i + 2$

- (3) (a) Schmidt, G. M. J.; Hodgkin, D. C.; Oughton, B. M. *Biochem. J.* **1957**, *65*, 744–756. (b) De Santis, P.; Liquori, A. M. *Biopolymers* **1971**, *10*, 699–710.

<sup>†</sup> Leiden Institute of Chemistry.

<sup>‡</sup> Universidad de Santiago de Compostela.

<sup>§</sup> National Institute of Public Health and the Environment.

<sup>||</sup> TNO.

<sup>‡</sup> Current address: Whitehead Institute for Biomedical Research, Nine Cambridge Center, Cambridge, MA 02142, USA.

(1) Gause, G. F.; Brazhnikova, M. G. *Nature* **1944**, *154*, 703.

(2) (a) Izumiya, N.; Kato, T.; Aoyagi, H.; Waki, M.; Kondo, M. *Synthetic aspects of biologically active cyclic peptides – gramicidin S and tyrocidines*; Halstead (Wiley): New York, 1979. (b) Waki, M.; Izumiya, N. *Biochemistry of Peptide Antibiotics*; Kleinhaug, H., van Doren, H., Eds.; Walter de Gruyter Company: Berlin, 1990. (c) Kondejewski, L. H.; Farmer, S. W.; Wishart, D. S.; Hancock, R. E. W.; Hodges, R. S. *Int. J. Peptide Protein Res.* **1996**, *47*, 460–466.

positions, respectively.<sup>4</sup> The observation that GS acts against the lipid bilayer itself and not against a specific cell membrane associated biomolecule is underscored by the finding that enantiomeric GS is equally active.<sup>5</sup> GS targets a broad range of bacteria depending on the type of bioassay, with solution-based microbiological screening assays showing greater activity against Gram-negative bacteria than gel-based assays.<sup>2c</sup> GS appears rather indiscriminate toward the nature of the lipid bilayer and kills mammalian cells with equal efficiency. For instance, GS displays potent hemolytic activity, and it is for this reason that the use of GS in human medicine is restricted to topical applications.<sup>2,6</sup>

Peptide antibiotics such as GS that target the lipid bilayer as a whole, and not a specific subcellular target, are of great interest in the search for new antibiotics.<sup>7</sup> In general, bacterial strains can readily become resistant against compounds that interfere with a specific metabolic process, or block a specific enzyme or receptor, by genetically altering the target such that it defies recognition.<sup>8</sup> Gaining resistance against GS would require a strategy that, for instance, specifically destroys it or blocks its accumulation in the lipid bilayer. Arguably, such alterations are less easily attained through genetic mutations, and it is for this reason that the search for nontoxic GS analogues and related cationic antimicrobial peptides has found wide attraction.<sup>9</sup> Obviously, this search can only be concluded successfully when compounds are identified that do act upon bacterial lipid bilayers but leave their mammalian counterparts untouched. For this to be possible it is of profound importance to understand the exact mode of action with which GS disrupts lipid bilayers. At present such detailed information is not available.

We have contributed to the field of GS-based antibiotics by the synthesis of analogues in which one of the two type II'  $\beta$ -turns is replaced with selected sugar amino acids (SAA).<sup>10</sup> SAAs are sugar peptide hybrids that combine monosaccharide properties (conformational rigidity, added functionalities) with

those of amino acids.<sup>11</sup> SAAs can be readily obtained and incorporated into oligopeptides as dipeptide isosteres. Our strategy is to analyze the conformational behavior of SAA modified GS analogues using both NMR and X-ray analysis and to correlate the results with toxicity studies toward both bacterial strains and red blood cells. In the course of these studies we observed an intriguing conformation in GS analogue **1**, containing a furanoid SAA at one of the turn regions.<sup>10b</sup> One of the two hydroxyl functionalities of the SAA moiety in **1** ( $C_3$ -OH) is involved in an intraresidue hydrogen bond leading to a distortion of the  $\beta$ -hairpin structure (Figure 1B), as compared to GS. Inspection of the molecular packing of **1** in its X-ray structure revealed a hexameric  $\beta$ -barrel-like structure composed of six crystallographically equivalent units of **1**, with the positively charged Orn side chains extending into the core and the Val, Leu, and <sup>D</sup>Phe residues forming a hydrophobic periphery (see Figure 1C). This hexameric  $\beta$ -barrel-like pore structure, the first of its kind, agrees with a molecular arrangement as suggested in a barrel stave type mechanism of membrane disrupting cationic antibiotic peptides.<sup>12</sup>

At first, our interest in this X-ray structure was dampened by the strongly reduced antibacterial activity displayed by **1**.<sup>10a</sup> We reasoned that the diminished biological activity of **1** compared to GS could be caused by either the altered  $\beta$ -hairpin structure or by the hydrophilic character of the SAA moiety as compared to the hydrophobic <sup>D</sup>Phe-Pro sequence in GS. As one of the hydroxyl groups of the SAA moiety of **1** is not involved in hydrogen bonding ( $C_4$ -OH), it can be modified to introduce an aromatic functionality, thus more closely resembling the hydrophobic nature of the original turn sequence. We here present a synthetic strategy that allows the facile introduction of aromatic functionality in the SAA turn region of **1** (GS analogues **10a-c**) and provide an in-depth structural analysis, as well as a biological evaluation. We show that analogues **10a-c** adopt the same distorted cyclic  $\beta$ -hairpin secondary structure as compound **1** but that the biological activity is comparable to that of the natural product, gramicidin S.

## Materials and Methods

**Abbreviations.** GS = gramicidin S, SAA = sugar amino acid.

**Synthesis.** Except when indicated otherwise, all reactions were performed under an inert atmosphere and at ambient temperature. All reagents were purchased from Aldrich, Acros, or Novabiochem and were used as supplied. CAUTION: Sodium azide is toxic and can explode when exposed to heat, pressure, or shock, particularly in combination with heavy metals or their salts. Organic azides, such as derivatives **3-6a-c**, can in principle also decompose explosively, and appropriate safety measures must therefore be taken at all times. Full details, including the characterization of the intermediates, are provided in the Supporting Information.

**Representative Alkylation Procedure.** Alcohol **3** (1.96 g, 8.55 mmol) was dissolved in DMF (40 mL) and cooled to 0 °C. To the solution were added benzyl bromide (1.124 mL, 9.4 mmol, 1.1 equiv) and sodium hydride (376 mg, 9.4 mmol, 1.1 equiv), and the mixture

- (4) Hull, S. E.; Karlsson, R.; Main, P.; Woolfson, M. M.; Dodson, E. J. *Nature* **1978**, *275*, 206–207.
- (5) Shemyakin, M. M.; Ovchinnikov, Y. A.; Ivanov, V. T.; Ryabova, I. D. *Experientia* **1967**, *23*, 326. (b) Goodman, M.; Chorev, M. *Acc. Chem. Res.* **1979**, *12*, 1–7.
- (6) Kondejewski, L. H.; Farmer, S. W.; Wishart, D. S.; Hancock, R. E. W.; Hodges, R. S. *Int. J. Peptide Protein Res.* **1996**, *47*, 460–466.
- (7) (a) Matsuzaki, K. *Biochim. Biophys. Acta* **1999**, *1462*, 1–10. (b) Epanand, R. M.; Vogel, H. J. *Biochim. Biophys. Acta* **1999**, *1462*, 11–28. (c) Sitaram, N.; Nagaraj, R. *Biochim. Biophys. Acta* **1999**, *1462*, 29–54. (d) Shai, Y. *Biochim. Biophys. Acta* **1999**, *1462*, 55–70. (e) Dathe, M.; Wieprecht, T. *Biochim. Biophys. Acta* **1999**, *1462*, 71–87. (f) Blondelle, S. E.; Lohner, K.; Aguilar, M.-I. *Biochim. Biophys. Acta* **1999**, *1462*, 89–108. (g) Maget-Dana, R. *Biochim. Biophys. Acta* **1999**, *1462*, 109–140. (h) Lohner, K.; Prenner, E. J. *Biochim. Biophys. Acta* **1999**, *1462*, 141–156. (i) Bechinger, B. *Biochim. Biophys. Acta* **1999**, *1462*, 157–183. (j) La Rocca, P.; Biggin, P. C.; Tieleman, D. P.; Sansom, M. S. P. *Biochim. Biophys. Acta* **1999**, *1462*, 185–200. (k) Prenner, E. J.; Lewis, R. N. A. H.; McElhaney, R. N. *Biochim. Biophys. Acta* **1999**, *1462*, 201–221. (l) Breukink, E. J.; de Kruijff, B. *Biochim. Biophys. Acta* **1999**, *1462*, 223–234.
- (8) Walsh, C. T. *Antibiotics: Actions, Origins, Resistance*; ASM: Washington, DC, 2003.
- (9) (a) Zasloff, M. *Nature* **2002**, *415*, 389–395. (b) Lee, D. L.; Hodges, R. S. *Biopolymers* **2003**, *71*, 28–48. (c) Bulet, P.; Stöcklin, R.; Menin, L. *Immunol. Rev.* **2004**, *198*, 169–184. (d) Finlay, B. B.; Hancock, R. E. W. *Nat. Rev. Microbiol.* **2004**, *2*, 497–504. (e) Lehrer, R. I. *Nat. Rev. Microbiol.* **2004**, *2*, 727–738.
- (10) (a) Grotenbreg, G. M.; Kronemeijer, M.; Timmer, M. S. M.; El Oualid, F.; van Well, R. M.; Verdoes, M.; Spalburg, E.; van Hooft, P. A. V.; de Neeling, A. J.; Noort, D.; van Boom, J. H.; van der Marel, G. A.; Overkleef, H. S.; Overhand, M. J. *Org. Chem.* **2004**, *69*, 7851–7859. (b) Grotenbreg, G. M.; Timmer, M. S. M.; Llamas-Saiz, A. L.; Verdoes, M.; van der Marel, G. A.; van Raaij, M. J.; Overkleef, H. S.; Overhand, M. J. *Am. Chem. Soc.* **2004**, *126*, 3444–3446. (c) Grotenbreg, G. M.; Christina, A. E.; Buizert, A. E. M.; van der Marel, G. A.; Overkleef, H. S.; Overhand, M. J. *J. Org. Chem.* **2004**, *69*, 8331–8339.

- (11) (a) Gervay-Hague, J.; Weathers, T. M. *J. Carbohydr. Chem.* **2002**, *21*, 867–910. (b) Schweizer, F. *Angew. Chem., Int. Ed.* **2002**, *41*, 230–253. (c) Gruner, S. A. W.; Locardi, E.; Lohof, E.; Kessler, H. *Chem. Rev.* **2002**, *102*, 491–514. (d) Chakraborty, T. K.; Srinivasu, P.; Tapadar, S.; Mohan, B. K. *J. Chem. Sci.* **2004**, *116*, 187–207.
- (12) (a) Oren, Z.; Shai, Y. *Biopolymers* **1998**, *47*, 451–463. (b) Shai, Y. *Biopolymers* **2002**, *66*, 236–248. (c) Yeaman, M. R.; Yount, N. Y. *Pharmacol. Rev.* **2003**, *55*, 27–55. (d) Brogden, K. A. *Nat. Rev. Microbiol.* **2005**, *3*, 238–250.

was stirred for 16 h. The reaction was quenched with methanol (5 mL) and concentrated in vacuo. The crude mixture was partitioned between saturated aqueous NaHCO<sub>3</sub> and EtOAc, and the aqueous layer was subsequently extracted with EtOAc twice. The combined organic layers were dried (MgSO<sub>4</sub>), filtered, and concentrated. Silica gel column chromatography (20%→30% EtOAc in light PE) yielded the azide **4a** (2.54 g, 7.95 mmol) in 93% as a transparent oil.

**Representative Methanolysis Procedure.** Isopropylidene-protected **4a** (1.6 g, 5.0 mmol) was dissolved in methanol (10 mL), and PPTS (~50 mg, cat) was added. The mixture was heated to 50 °C and stirred for 16 h. The reaction was next diluted with EtOAc, extracted with saturated aqueous NaHCO<sub>3</sub>, dried (MgSO<sub>4</sub>), filtered, and evaporated to dryness. Silica gel column chromatography (50%→70% EtOAc in light PE) produced diol **5a** (0.945 g, 3.39 mmol) in 68% as a white amorphous solid.

**Representative Oxidation Procedure.** Diol **5a** (474 mg, 1.70 mmol) was dissolved in acetonitrile (10 mL) after which saturated aqueous NaHCO<sub>3</sub> (4 mL) containing KBr (~20 mg, cat) was added, and the mixture was cooled to 0 °C. Subsequently, TEMPO catalyst (5 mg) in acetonitrile (3 mL) was added, and a premixed solution of 15% NaOCl (7.5 mL, 1.80 mmol), in saturated aqueous NaHCO<sub>3</sub> (4.5 mL) and saturated aqueous NaCl (8.8 mL), was added dropwise to the reaction mixture, keeping it oscillating between yellow and colorless. The reaction was then quenched with MeOH, acidified to pH = 4 with HCl (1 mL), and extracted with DCM thrice. The combined organic layers were dried (MgSO<sub>4</sub>), filtered, and evaporated. Silica gel column chromatography (20%→30% EtOAc in light PE) quantitatively furnished SAA **6a** (507 mg, 1.70 mmol) as a transparent oil.

**Peptide Synthesis.** Resin **7** was prepared as reported earlier<sup>10a</sup> and was elongated by repetitive removal of the Fmoc protecting group and coupling of the next amino acids under standard conditions. Final coupling of **6a**, **6b**, or **6c** (0.2 mmol, 2 equiv), BOP (132 mg, 0.3 mmol, 3 equiv), HOBt (41 mg, 0.3 mmol, 3 equiv), and DiPEA (58  $\mu$ L, 0.35 mmol, 3.5 equiv) in NMP (2 mL) gave the immobilized azides **8a–c**. The resins were then dispersed in 1,4-dioxane (10 mL) to which trimethylphosphine (1.6 mL, 1.6 mmol, 1 M in toluene, 16 equiv) and water (1 mL) were added. After shaking for 4 h, the solid phase was washed, and the resulting peptides were released from the resin (1% TFA in DCM) and cyclized by dropwise addition to a vigorously stirred solution of PyBOP (5 equiv), HOBt (5 equiv), and DiPEA (15 equiv) to furnish the compound **9a** (116 mg, 86  $\mu$ mol, 86%), **9b** (80 mg, 56  $\mu$ mol, 56%), and **9c** (137 mg, 98  $\mu$ mol, 98%), respectively, as white amorphous solids, after size exclusion chromatography. The Boc-protected peptides **9a** (58 mg, 43  $\mu$ mol), **9b** (20 mg, 14  $\mu$ mol), and **9c** (11.6 mg, 8.3  $\mu$ mol) were dissolved in DCM (2 mL) and cooled to 0 °C. The mixtures were subsequently treated with TFA (2 mL), stirred for 30 min, and diluted with toluene (10 mL), after which the volatiles were removed in vacuo. The crude products were purified by semi-preparative HPLC to give, after lyophilization, **10a–c** in 87%, 34%, and 57% yield, respectively.

**X-ray Crystallography.** Lyophilized peptide **10c** (0.89 mg, 0.74  $\mu$ mol) was dissolved in 75  $\mu$ L of MeOH/H<sub>2</sub>O (2/1, v/v), after which aliquots of 5  $\mu$ L of the solution were pipetted into a 96-well microtiter plate (Terasaki plate) under a layer of *n*-decane. To the sample, 5  $\mu$ L of different crystallization solutions were added, after which the *n*-decane layer was replaced with paraffin oil. The microtiter plate was allowed to stand at 20 °C. Crystals developed at several conditions. A crystal grown in 15% (v/v) 2-methyl-2,4-pentanediol, 50 mM sodium acetate, and 10 mM calcium chloride (pH 4.6) was mounted in a cryoloop and frozen in liquid nitrogen. A complete dataset was collected at ESRF (Grenoble, France) at beamline ID23-1 from one crystal (0.24  $\times$  0.08  $\times$  0.06 mm<sup>3</sup>) at 100 K using an oscillation camera equipped with an MAR Mosaic CCD detector. A total of 329 oscillation images were taken in three runs. Data were processed using HKL Denzo<sup>13</sup> and SORTAV.<sup>14</sup> The structure was solved by direct methods (SIR2002<sup>15</sup>)

and refined with full-matrix least-squares analysis on  $F^2$  using SHELXL-97.<sup>16</sup> Of the reflections, 5% were flagged to compute the Rfree except for the last refinement cycles where all reflection were included to calculate the final esd for the refined parameters and the R1 and wR2 values. Due to the limited resolution of 1.0 Å, the partial disorder of the peptide, and the presence of very big solvent channels in the crystal, hydrogen atoms could not be localized for the ordered water solvent molecules. All non-H atoms were refined anisotropically (for data and refinement statistics, see Supporting Information). CCDC 278146 contains the supplementary crystallographic data for this structure. These data can be obtained free of charge via [www.ccdc.cam.ac.uk/conts/retrieving.html](http://www.ccdc.cam.ac.uk/conts/retrieving.html) (or from the Cambridge Crystallographic Data Centre, 12 Union Road, Cambridge CB21EZ, UK).

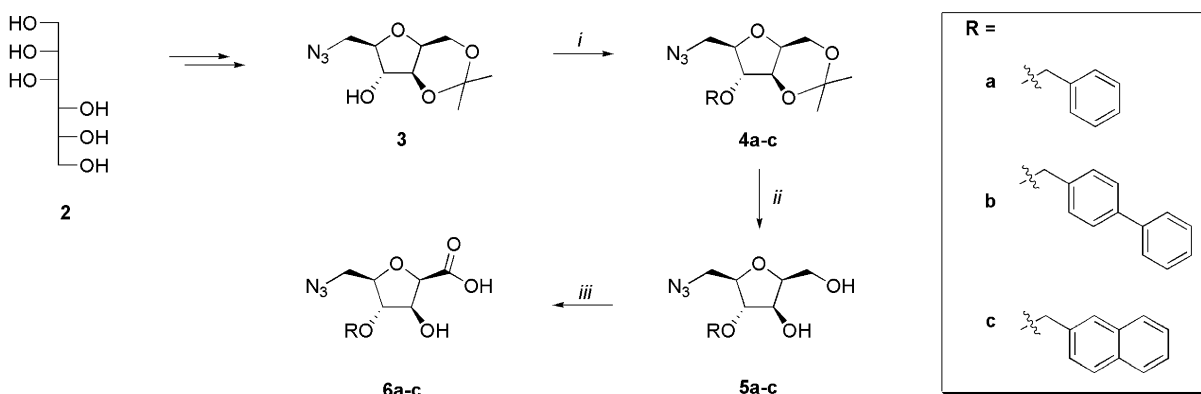
**Antibacterial Activity.** The following bacterial strains were used: *Staphylococcus aureus* (ATCC 29213), *Staphylococcus epidermidis* (ATCC 12228), *Enterococcus faecalis* (ATCC 29212), *Bacillus cereus* (ATCC 11778), *Escherichia coli* (ATCC 25922), and *Pseudomonas aeruginosa* (ATCC 27853). Bacteria were stored at –70 °C and grown at 35 °C on Columbia Agar with sheep blood (Oxoid, Wesel, Germany) overnight and diluted in 0.9% NaCl. Microtiter plates (96 wells of 100  $\mu$ L) as well as large plates (25 wells of 3 mL) were filled with Mueller Hinton II Agar (Becton Dickinson, Cockeysville, USA) containing serial 2-fold dilutions of peptides **10a–c**. To the wells were added 3  $\mu$ L of bacteria, to give a final inoculum of 10<sup>4</sup> colony forming units (CFU) per well. The plates were incubated overnight at 35 °C and the MIC was determined as the lowest concentration inhibiting bacterial growth.

**Hemolytic Activity.** The hemolytic activity of the peptides was determined in quadruple. Human blood was collected into EDTA tubes and centrifuged to remove the buffy coat. The residual erythrocytes were washed 3 times in 0.85% saline. Serial 2-fold dilutions of the peptides **10a–c** in saline were prepared in sterilized round-bottom 96-well plates (polystyrene, U-bottom, Costar) using 100  $\mu$ L volumes (500–0.5  $\mu$ M). Red blood cells were diluted with saline to 1/25 packed volume of cells, and 50  $\mu$ L of the resulting cell suspension were added to each well. Plates were incubated while gently shaking at 37 °C for 4 h. Next, the microtiter plate was quickly centrifuged (1000 g, 5 min), and 50  $\mu$ L of supernatant of each well were transported into a flat-bottom 96-well plate (Costar). The absorbance was measured at 405 nm using an mQuant microplate spectrophotometer (Bio-Tek Instruments). The  $A_{\text{blank}}$  was measured in the absence of additives and 100% hemolysis ( $A_{\text{tot}}$ ) in the presence of 1% Triton X-100 in saline. The percentage hemolysis is determined as  $(A_{\text{pep}} - A_{\text{blank}})/(A_{\text{tot}} - A_{\text{blank}}) \times 100$ .

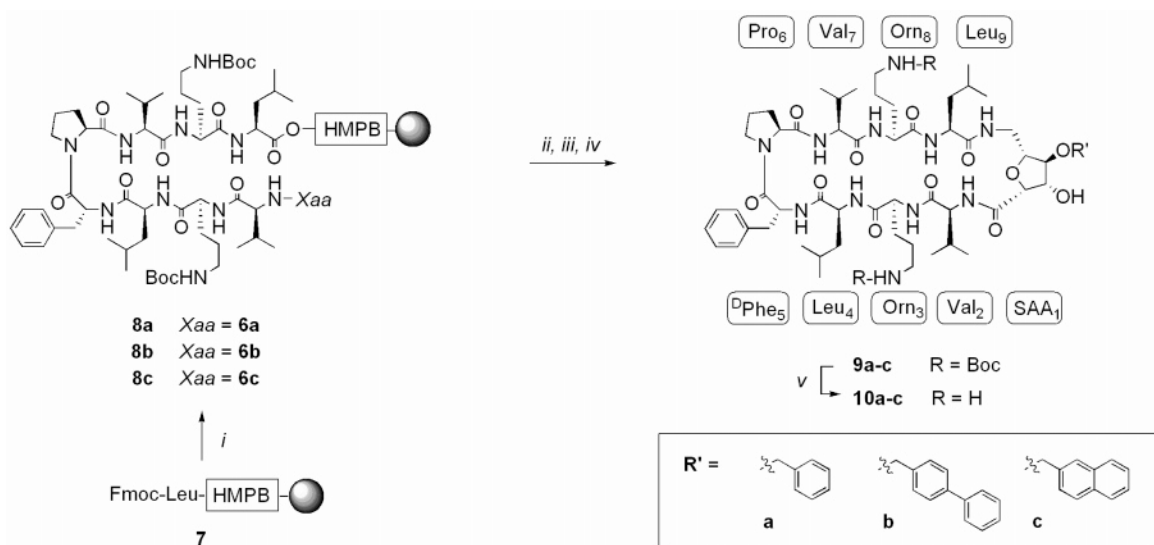
## Results

**Synthesis.** The synthesis of GS analogues **10a–c** commenced with the preparation of arylated SAA building blocks SAAs **6a–c** as follows. 2,5-Anhydroglucitol **3** (Scheme 1), readily prepared from D-mannitol **2** following the literature procedure,<sup>17</sup> was alkylated with benzyl bromide, 4-biphenylmethyl bromide, and naphthyl bromide, respectively, under the agency of sodium hydride to furnish **4a** (93%), **4b** (89%), and **4c** (77%). The naphthylmethyl- and biphenylmethyl bromides required for the preparation of **4b** and **4c** were prepared from their corresponding

- (13) Otwinowski, Z.; Minor, W. *Methods in Enzymology, Volume 276: Macromolecular Crystallography, Part A*; Carter, C. W., Jr., Sweet, R. M., Eds.; Academic Press: 1997; pp 307–326.
- (14) Blessing, R. H. *Acta Crystallogr.* **1995**, *A51*, 33–38.
- (15) Burla, M. C.; Camalli, M.; Carrozzini, B.; Cascarano, G. L.; Giacovazzo, C.; Polidoria, G.; Spagna, R. *J. Appl. Crystallogr.* **2003**, *36*, 1103.
- (16) Sheldrick, G. M. *SHELX97*; University of Göttingen: Germany, 1997.
- (17) Timmer, M. S. M.; Verdoes, M.; Slidregt, L. A. J. M.; van der Marel, G. A.; van Boom, J. H.; Overkleeft, H. S. *J. Org. Chem.* **2003**, *68*, 9406–9411.

**Scheme 1.** Synthesis of the Sugar Amino Acids<sup>a</sup>

<sup>a</sup> (i) NaH (1.1 equiv), RBr (1 equiv), DMF, 0 °C, 16 h, **4a**, 93%; **4b**, 89%; **4c**, 77%; (ii) PPTS (cat.), MeOH, 50 °C, 16 h, **5a**, 68%; **5b**, 58%; **5c**, 69%; (iii) TEMPO (cat.), NaOCl, NaHCO<sub>3</sub> (aq), MeCN, 0 °C, **6a**, quant; **6b**, 52%; **6c**, 72%.

**Scheme 2.** Synthesis of the GS Analogues<sup>a</sup>

<sup>a</sup> (i) Fmoc deprotection: piperidine/NMP (1/4 v/v), condensation: Fmoc-aa-OH (3 equiv) or SAA, **6a**, **6b**, and **6c** (2 equiv), BOP (3 equiv), HOBt (3 equiv), DiPEA (3.3 equiv), NMP, 90 min; (ii) PMe<sub>3</sub> (16 equiv), 1,4-dioxane/H<sub>2</sub>O (10/1 v/v); (iii) TFA/DCM (1/99 v/v), 4 × 10 min; (iv) PyBOP (5 equiv), HOBt (5 equiv), DiPEA (15 equiv), DMF, 16 h, **9a**, 86%; **9b**, 56%; **9c**, 98%; (v) TFA/DCM (1/1 v/v) 30 min, **10a**, 87%; **10b**, 34%; **10c**, 57%.

alcohols.<sup>18</sup> Cleavage of the isopropylidene group using a catalytic amount of pyridinium *p*-toluenesulfonate (PPTS) gave diols **5a–c** in their respective yields of 68%, 58%, and 50%. Oxidation of the primary alcohol in **5a–c**, employing a catalytic amount of TEMPO (2,2,6,6-tetramethyl-piperidinyl-1-oxy) and NaOCl as co-oxidant, afforded SAAs **6a** (quant.), **6b** (52%), and **6c** (72%), respectively.

Next, the assembly of **10a–c** was undertaken (Scheme 2). MBHA-resin **7**, functionalized with the acid-labile HMPB-linker system, was condensed with Fmoc-Leu-OH and further elongated using standard Fmoc-based SPPS protocols. The N-terminal azides of the immobilized nonapeptides **8a–c** were subjected to Staudinger reduction, and the resulting peptides were released from the resin (1% TFA in DCM) and cyclized by dropwise addition to a vigorously stirred solution of PyBOP (5 equiv), HOBt (5 equiv), and DiPEA (15 equiv). Size exclusion chromatography gave the fully protected **9a** (86%), **9b** (56%), and **9c** (98%), respectively. Removal of the Boc protective groups and HPLC purification furnished homoge-

neous GS analogues **10a** (87%), **10b** (34%), and **10c** (57%), respectively.

**NMR Analysis.** The unambiguous <sup>1</sup>H NMR resonance assignment of each peptide was performed using COSY, TOCSY, and NOESY or ROESY experiments. The large resonance distribution, indicative of secondary structure formation, allowed complete assignment of the data sets of peptides **10a–c**. To aid in identifying the presence of secondary structure elements, the vicinal spin–spin coupling constants<sup>19</sup> of the amide bonds (<sup>3</sup>J<sub>H<sub>N</sub>α</sub>, Figure 2A) and the chemical shift perturbation<sup>20</sup> of the H<sub>α</sub> of individual amino acid residues (ΔδH<sub>α</sub>, Figure 2B) were compared to those found in native GS. The distinctive trends found in these data were largely comparable to GS and **1** and consistent with a β-sheet structure.<sup>10</sup>

The preservation of the β-sheet structure in benzyl-derivative **10a** was further corroborated by the observation of interstrand NH–NH NOEs, such as Val<sub>2</sub>–Leu<sub>9</sub> (NOE **b**, Figure 3) and Val<sub>7</sub>–

(18) Brun, K. A.; Linden, A.; Heimgartner, H. *Helv. Chim. Acta* **2002**, *85*, 3422–3443.

(19) Wüthrich, K. *NMR of Proteins and Nucleic Acids*, John Wiley & Sons: New York, 1986.

(20) Wishart, D. S.; Sykes, B. D.; Richards, F. M. *Biochemistry* **1992**, *31*, 1647–1651.

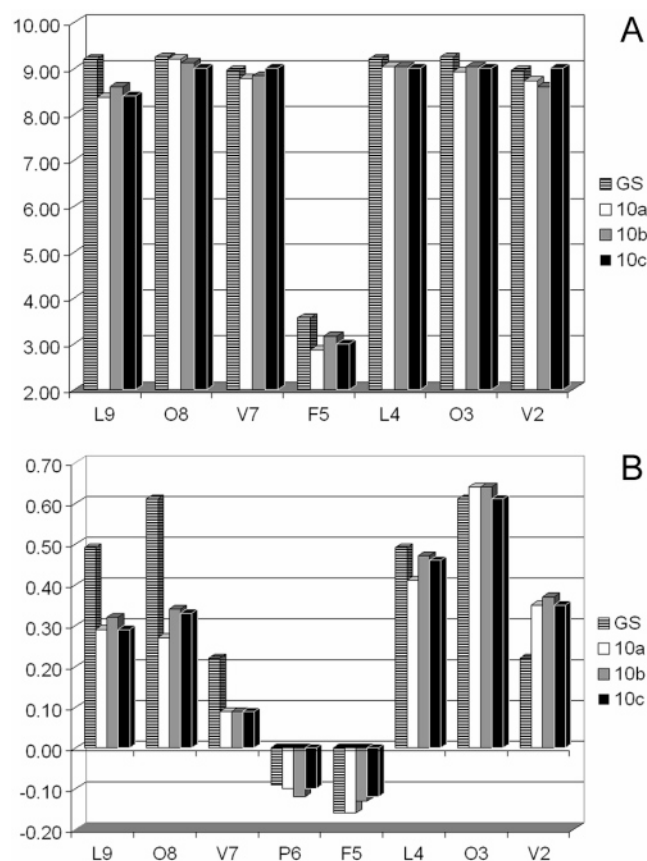


**Figure 2.** NMR analysis of SAA-modified GS analogues **10a–c**. (A) Coupling constants ( $^3J_{\text{HN}\alpha}$ ). (B) The chemical shift perturbations ( $\Delta\delta H_\alpha = \text{observed } \delta H_\alpha - \text{random coil } \delta H_\alpha$ ).

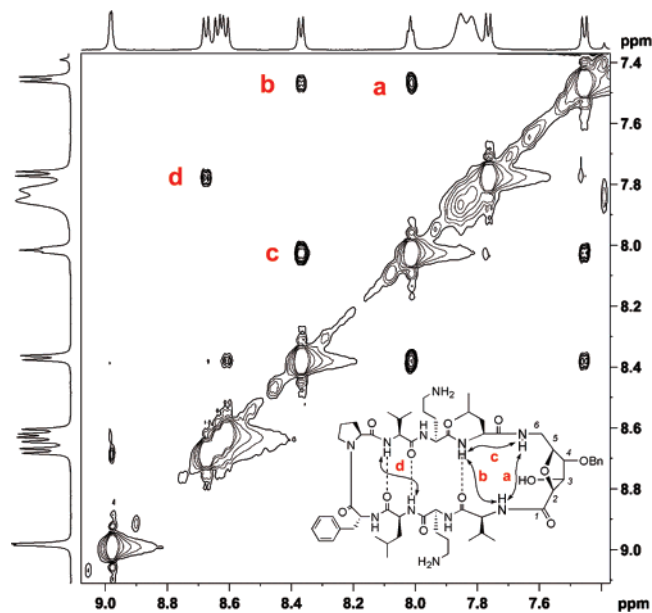


**Figure 3.** Amide region of the ROESY spectrum (600 MHz,  $\text{CD}_3\text{OH}$ ) of peptide **10a**.

Leu<sub>4</sub> (NOE **d**), as well as the sequential NH–NH cross-peak of SAA<sub>1</sub>–Leu<sub>9</sub> (NOE **c**). Moreover, the characteristic NOE contact between SAA<sub>1</sub>–NH and its neighboring Val<sub>2</sub>–NH was discerned (NOE **a**, Figure 3), providing evidence that the structure adopted by **1**, as observed through  $^1\text{H}$  NMR and single-crystal X-ray analysis, was again assumed by aromatic GS

analogue **10a**. Similar observations through spectroscopic comparison were made for biphenyl- and naphthyl-functionalized **10b** and **10c**, respectively. Thus, the monoarylated SAAs **6a–c** appear to induce the same reverse turn conformation in GS analogues **10a–c** in solution as the fully hydroxylated SAA moiety does in GS analogue **1**.

**X-ray Analysis.** Buffered aqueous solutions of **10c** were allowed to evaporate slowly under oil. After 4 months, crystals of **10c** developed, and the crystal structure of one of them was solved by X-ray diffraction (Figure 4A). This provided final confirmation, in line with our spectroscopic data, that the peptide indeed adopts a  $\beta$ -sheet structure with a distinctive reverse turn that is identical to **1** (Figure 1B). Inspection of the molecular packing of a single unit cell revealed a porelike assembly comprised of 12 individual cyclic peptides (Figure 4B). Peptide monomers related by a binary axis perpendicular to the pore channel form dimers (Figure 4C). Six of these dimers, arranged in a helix, give rise to a complete turn of the helical pore. This pore subsequently forms an infinite helical tube displaying 6<sub>5</sub> screw axis symmetry. The pore assemblies of **10c**, those observed in the molecular packing of a hydrated GS–urea complex (Figure 4D),<sup>21</sup> and GS–trifluoroacetic acid–HCl (Figure 4E) are all helical motifs and are distinct to the stacking of hexameric barrels displayed by **1** (Figure 4F). For example, the  $\beta$ -strands of the cyclic peptide units **10c** are almost perpendicular with the axis of the pore, whereas the  $\beta$ -strands of **1** are closer to a parallel orientation with respect to the pore axis. Moreover, the assembly of **10c** (Figure 4B) forms a larger pore than the assembly of **1** (Figure 1C). However, all assemblies are similar with respect to their hydrophilic interior and hydrophobic exterior.

**Antibacterial and Hemolytic Activity.** The bactericidal activity of GS analogues **10a–c** against a number of Gram-positive and -negative strains was evaluated (Table 1). The Gram-positive strains *S. aureus*, *S. epidermidis*, *E. faecalis*, and *B. cereus* proved to be highly sensitive toward the GS analogues **10a–c**, with MIC values comparable to those observed for native GS. As we had established earlier,<sup>10a</sup> the nonarylated GS analogue **1** was largely inactive against all bacterial strains included in the assay. The Gram-negative *E. coli* and *P. aeruginosa* strains proved resistant to the action of **10a–c**, as well as to GS.<sup>2c</sup> The nature of the aromatic appendage from the SAA does not influence the biological profile, as the benzyl, biphenyl, and naphthyl derivatives proved to be equally active. The hemolytic properties of peptides **10a–c** toward human erythrocytes were similarly assessed and compared to those of native GS (Figure 5).

Peptides **10a–c** show a similar toxicity compared to GS that is not influenced by the difference in aromatic moieties, as the benzyl, biphenyl, and naphthyl derivatives display comparable hemolytic profiles. These data demonstrate that the advantageous effect of aromatic decoration of the SAAs on the capacity of peptides **10a–c** to arrest proliferation of various strains of bacteria concurrently increases the toxicity toward human erythrocytes.<sup>22</sup>

- (21) Tishchenko, G. N.; Andrianov, V. I.; Vainstein, B. K.; Woolfson, M. M.; Dodson, E. *Acta Crystallogr.* **1997**, *D53*, 151–159.  
 (22) Several less toxic GS analogues have been reported: (a) Ando, S.; Nishikawa, H.; Takiguchi, H.; Lee, S.; Sugihara, G. *Biochim. Biophys. Acta* **1993**, *1147*, 42–49. (b) Lee, D. L.; Hodges, R. S. *Biopolymers* **2003**, *71*, 28–48. (c) Kawai, M.; Yamamura, H.; Tanaka, R.; Umemoto, H.; Ohmizo, C.; Higuchi, S.; Katsu, T. *J. Pept. Res.* **2005**, *65*, 98–104.

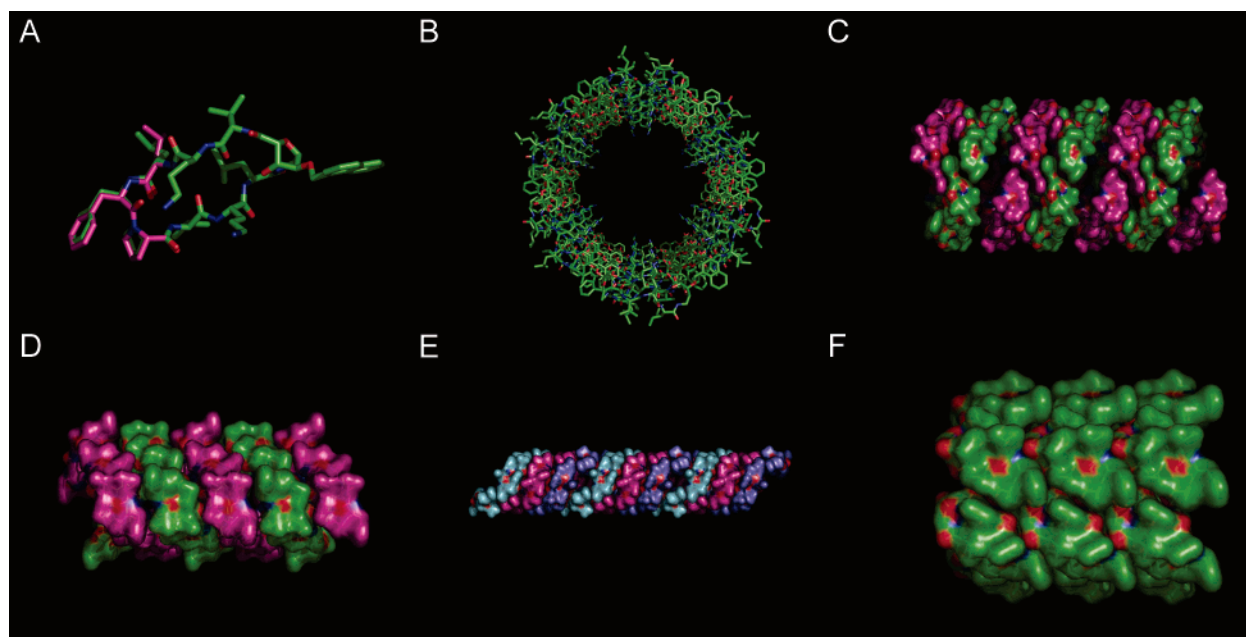


**Figure 4.** (A) Monomeric X-ray structure of **10c**. (B) The molecular packing of **10c** along the pore axis. (C) The dodecameric helical assembly viewed perpendicular to the pore. (D) The hexameric helical assembly of the GS–urea complex. (E) The nonameric helical assembly of the GS–TFA–HCl complex. (F) The hexameric barrel of **1**. Solvent and water molecules have been omitted for clarity.

**Table 1.** Antimicrobial Activity (MIC in  $\mu\text{g/mL}$ ) of Peptides **10a–c** in Comparison to GS<sup>a</sup>

peptide	<i>S. aureus</i> <sup>b</sup>		<i>S. epidermidis</i> <sup>b</sup>		<i>E. faecalis</i> <sup>b</sup>		<i>B. cereus</i> <sup>b</sup>		<i>E. coli</i> <sup>c</sup>		<i>P. aeruginosa</i> <sup>c</sup>	
	25W <sup>d</sup>	MT <sup>e</sup>	25W <sup>d</sup>	MT <sup>e</sup>	25W <sup>d</sup>	MT <sup>e</sup>	25W <sup>d</sup>	MT <sup>e</sup>	25W <sup>d</sup>	MT <sup>e</sup>	25W <sup>d</sup>	MT <sup>e</sup>
GS	4	4	2	2	8	8	4	4	>64	64	>64	>64
<b>10a</b>	8	2	2	2	16–32	16	4	4	64	64	>64	>64
<b>10b</b>	8	8	2	4	16	8–16	8	8	>64	>64	>64	>64
<b>10c</b>	4–8	4	2	4	8	8	4	4	>64	>64	>64	>64

<sup>a</sup> Measurements were executed using standard agar 2-fold dilution techniques. <sup>b</sup> Gram-positive. <sup>c</sup> Gram-negative. <sup>d</sup> 3 mL/25 well plates. <sup>e</sup> 100  $\mu\text{L}$ /96 microtiter plates.

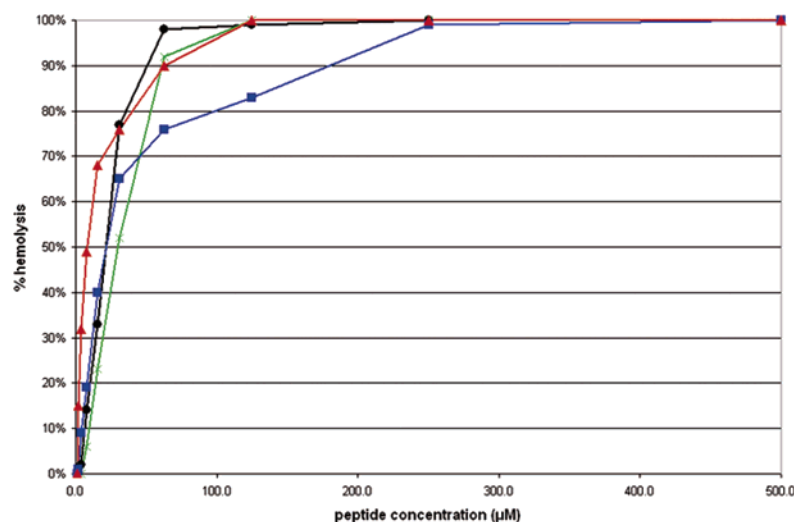


**Figure 5.** Hemolytic activity of GS analogues **10a–c** in comparison with GS.

## Discussion

GS analogue **1**, the intriguing structure of which we have reported previously and that exhibits limited antibacterial activity, formed the basis for the design of a new series of aromatic SAA-containing GS analogues **10a–c**. All three cyclic peptides **10a–c** adopt a  $\beta$ -sheet structure with the SAAs occupying a distinctive reverse turn analogous to peptide **1**,

irrespective of the aromatic group appended. Examination of the biological activity revealed that the antibacterial properties of the aromatic SAA-containing GS analogues was completely restored to the level of the parent compound GS, with a concomitant increase in hemolytic activity. We conclude that the presence of aromatic functionality in the turn region of these GS derivatives is a requirement for antibacterial activity.

Alteration of the conformation of one of the turns of GS is allowed with respect to the biological activity as long as this modified turn contains an aromatic functionality. This finding strongly suggests an important role of the aromatic functionalities in the mechanism of action of membrane disruption by GS.

At this point we cannot correlate conclusively the molecular packing of SAA analogues of GS, as observed in the X-ray structure, with their biological properties. However, we do believe it is striking that the active compounds so far analyzed (**10c** and native GS) form helical pores in crystals, while the less active compound **1** forms stacks of  $\beta$ -barrels. The work presented here encourages further efforts to design and synthesize alternate compounds to deepen our understanding of the structural requirements for biological activity of GS and related cationic antibiotic peptides, with the ultimate goal to arrive at GS analogues that target bacterial strains but are inactive against human blood cells.

**Acknowledgment.** This work was financially supported by the Council for Chemical Sciences of The Netherlands Organization for Scientific Research (CW-NWO), The Netherlands Technology Foundation (STW), and DSM Research. Kees Erkelens and Fons Lefeber are gratefully acknowledged for assistance with NMR experiments. We thank Nico Meeuwenoord and Hans van den Elst for their technical assistance. We thank Dr. David Hall for help with crystallographic data collection. A.L.L.-S. and M.J.v.R. also thank the Spanish Ministry of Education and Science for research funding and a Ramón y Cajal research fellowship to M.J.v.R.

**Supporting Information Available:** Detailed experimental procedures, compound characterization data, and experimental data for crystal structure determination of GS analogue **10c**. This material is available free of charge via the Internet at <http://pubs.acs.org>.

JA0588510